JACS
JOURNAL OF THE AMERICAN CHEMICAL SOCIETY

Article

pubs.acs.org/JACS

Magnetic-Directed Assembly from Janus Building Blocks to Multiplex Molecular-Analogue Photonic Crystal Structures

Su-Na Yin, Shengyang Yang, Cai-Feng Wang, and Su Chen*

The State Key Laboratory of Materials-Oriented Chemical Engineering and College of Chemistry and Chemical Engineering, Nanjing Tech University (former: Nanjing University of Technology), Nanjing 210009, People's Republic of China

Supporting Information

ABSTRACT: The predictable assembly of colloidal particles into a programmable superstructure is a challenging and vital task in chemistry and materials science. In this work, we develop an available magnetic-directed assembly strategy to construct a series of molecular-analogue photonic crystal cluster particles involving dot, line, triangle, tetrahedron, and triangular bipyramid configurations from solid–liquid Janus building blocks. These versatile multiplex molecular-analogue structural clusters containing photonic band gap, fluorescent, and magnetic information can open a new promising access to a variety of robust hierarchical microstructural particle materials.

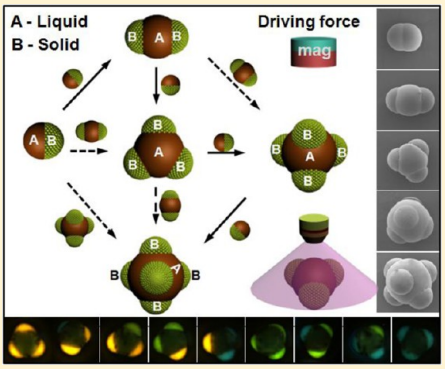

INTRODUCTION

There is a growing explosion in the synthesis of anisotropic particles because of their importance in various applications, such as optoelectronics, drug delivery, information storage, and biosensing.[1−8] Like molecules formed by atoms, anisotropic particles with diverse components and structures can be achieved from different building blocks to obtain distinct functions. To be specific, the elegant and exciting progress on particle-based self-assembly guarantees some micro- and nanoscale colloidal particles to be used as ingredients for the construction of anisotropic complex architectures or cluster structures, similar to the relationship between atoms and molecules.[9−17] Despite the absence of efficient valence and bonding between colloidal assemblies, those colloidal particles, with sizes varying from nanometers to several micrometers, can be integrated into anisotropic superstructural ensembles via specific directional interactions,[18−23] including chemical patchiness,[24−27] solution guide,[28−30] and surface template.[31,32] Therefore, tremendous interest is evoked in pioneering new building blocks toward the development of functional materials with collective properties and controllable anisotropy, which, however, is still a great challenge.

As a solution, microfluidic technique has been adequately employed to fabricate monodisperse photonic crystal (PC) supraparticles with single,[33] Janus,[34] capsule,[35] or even diverse compartments,[36,37] which are promising for applications such as biological analysis,[38] optical devices,[39] and chemical sensors.[40] Among those reported, however, most of the PC particles were of spherical geometry, which show either unique geometry but single component, or simple structure with different components. Apparently, PC particles with hierarchical microarchitectures or complex geometry are currently not realized. Meanwhile, efficient pathways are highly needed to selectively endow PCs with versatile collective functions while preserving their original optical properties.

In this work, we demonstrate an operable magnetic-directed assembly strategy to engineer PC particles into a series of molecular-analogue superstructural morphologies based on Janus building blocks. Herein, Janus building block composed of colloid PCs as the solid hemisphere and superparamagnetic nanoparticles confined in the other liquid part can be successfully designed via triphase microfluidics. Importantly, diverse functions can be integrated into the colloid PCs hemispheres of the Janus building block by loading fluorescent dyes or quantum dots (QDs), whereas the superparamagnetic liquid hemispheres allow the formation of hierarchical anisotropic structures via their coalescence upon collision under externally magnetic field, which confer the resulting materials on remote-controlled locomotion function. Therefore, the notable characteristics of solid–liquid phases within a single unit for particle synthesis would pave a new powerful way for the realization of advanced multifunctional materials. Moreover, with the use of solid–liquid Janus units as new building blocks, the first examples of molecular-analogue PC clusters including dot, line, triangle, tetrahedron, and triangular bipyramid structures were demonstrated, which are meaningful for various applications such as optoelectronic devices, combined sensors, encoding, and anticounterfeiting.

Received: September 24, 2015
Published: December 26, 2015

DOI: 10.1021/jacs.5b10039
J. Am. Chem. Soc. 2016, 138, 566−573

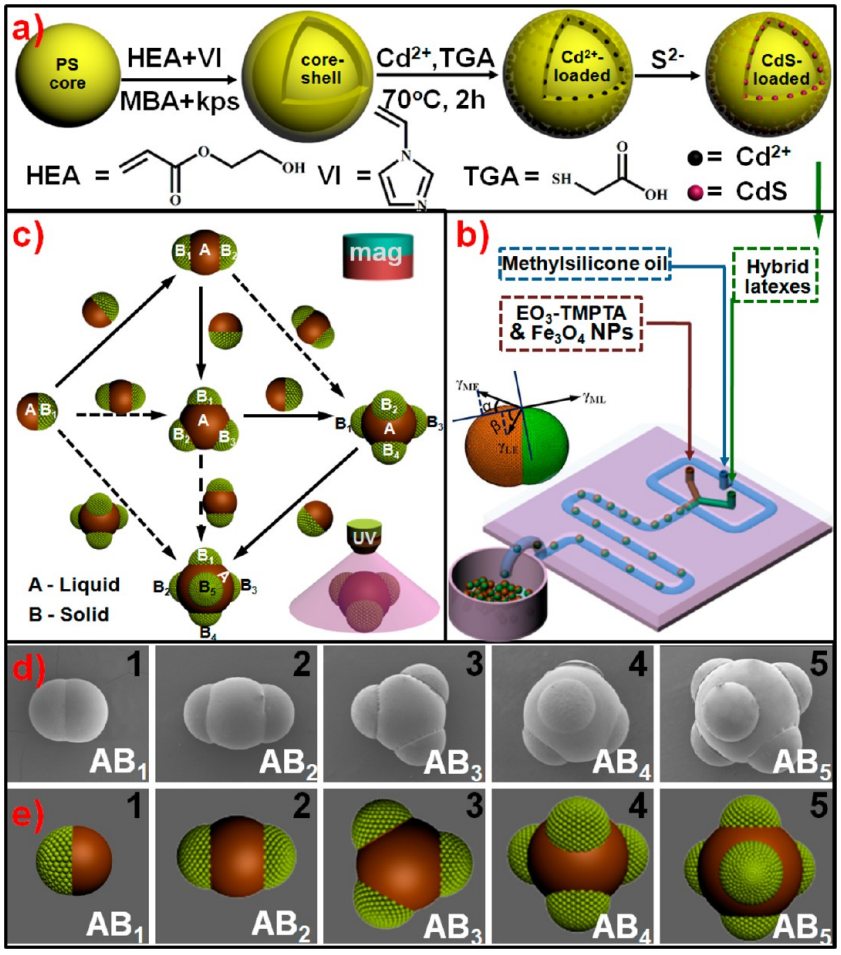

Figure 1. Anisotropic photonic crystal clusters constructed from solid–liquid Janus building blocks. (a) The chemical synthesis route toward QDs-loaded hybrid latexes. The prepared poly(styrene-*co*-2-hydroxyethyl acrylate) (PS-*co*-PHEA) was used as core to construct the shell of poly(*N*-vinylimidazole-*co*-2-hydroxyethyl acrylate) (PVI-*co*-PHEA), which could coordinate to cadmium ions, followed by the reaction with sulfide ions to form CdS QDs. (b) Schematic representation of a microfluidic process for the fabrication of solid–liquid Janus building blocks, where two independent phases containing hybrid latexes and EO_3-TMPTA and Fe_3O_4 nanoparticles initially generate discontinuous biphasic phase that intersects with continuous phase methylsilicone oil to build a periodic flow of double-faced droplets in oil. (c) Network of assembly pathways of complicated and symmetrical PC clusters formed from Janus building blocks based on the principle of lowest energy. Solid and dashed arrows denote the assembly mechanisms of Janus building blocks and clusters fusion, respectively. (d) Scanning electron microscope (SEM) image and (e) the model of diverse structures of magnetic-fluorescent PC clusters.

EXPERIMENTAL SECTION

Chemicals and Materials. Styrene (St) and *N*-vinylimidazole (VI) were purified by distillation under reduced pressure to remove inhibitors. The initiator, potassium persulfate (KPS), was purified by recrystallization from water twice and stored in a freezer before use. Methylsilicone oil used in this study was purchased from Dow Corning Corp. Purified water with resistance greater than 18 MΩ cm was used in our experiments. All other reagents were of analytical grade, purchased from standard sources, and used as received.

Synthesis of Pure Polystyrene (PS) Microspheres. Monodispersed PS microspheres were prepared according to our previous work.[39,41] The synthesis process was performed with a typical emulsion polymerization as follows: 7.5 g of St and 0.20 g of polyvinylpyrrolidone (PVP) were dissolved in 135 g of deionized water in a 250 mL round flask with stirring under nitrogen atmosphere. After the mixture was heated at 98 °C for 30 min, 0.04 g of KPS dissolved in 15 g of DI water was slowly added into a flask to initiate polymerization, and the reaction was continued for another 2 h.

Synthesis of Monodispersed Hydrogel Microspheres. Monodispersed hydrogel microspheres were synthesized according to our previous work,[42] with a typical seeded copolymerization as follows: 6.5 g of St, 1 g of HEA, and 0.20 g of PVP were dissolved in 135 g of DI water in a 250 mL round flask under stirring with nitrogen protection. After the mixture was heated at 98 °C for 30 min, polymerization was initiated by adding 0.04 g of KPS dissolved in 15 g of DI water. The reaction was kept for 2.5 h under constant stirring to obtain PS-*co*-PHEA seeds, and then 0.5 g of HEA, 0.5 g of VI, 0.002 g of MBA, and 0.005 g of KPS were added, and the reaction was continued for another 4 h.

Synthesis of CdS-Loaded Hybrid Microspheres. Monodispersed CdS-loaded hybrid microspheres were synthesized as follows: 0.5 g of the as-obtained monodispersed hydrogel microspheres was dispersed into the 30 g aqueous solution containing 0.2248 g of $CdCl_2 \cdot 2.5H_2O$ and 0.1842 g of TGA under stirring for 4 h at 70 °C to obtain the Cd^{2+}-doped microspheres. The excess Cd^{2+} ions then were removed by centrifugation and redispersion in DI water three times. Finally, the pH value was adjusted to 7 via 1 M NaOH solution, and 0.0128 g of $Na_2S \cdot 9H_2O$ dissolved in 5 mL of DI water was introduced to react with Cd^{2+} ions for about 3 h, gaining the final CdS-loaded hybrid latex. The products were further purified by centrifugation at 15 000 rpm to remove minor CdS QDs, which were weakly attached on the surface.

Preparation of Solid–Liquid Janus Building Blocks. Solid–liquid Janus building blocks were fabricated by a triphase microfluidic device. The microfluidic device was fabricated by inserting paired capillaries with 30 G needle into a polydimethylsiloxane (PDMS) tube (1.8 mm),

DOI: 10.1021/jacs.5b10039
J. Am. Chem. Soc. 2016, 138, 566–573

which forced three different solutions to flow simultaneously. Typically, a solution of 40 wt % CdS-loaded hybrid latex together with a photopolymerizable monomer of trimethylolpropane-ethoxylatetriacrylate (EO_3-TMPTA) containing Fe_3O_4 nanoparticles (2 wt %) and 2-hydroxy-2-methyl-1-phenyl-1-propanone (5 wt %) as a photoinitiator were introduced into the internal needles, respectively, at independently adjustable flow velocities by microinjection pumps. The PS solution was emulsified by 15 wt % of Triton X-100. Methylsilicone oil was introduced into the external PDMS capillary as the continuous phase. Flow rates were kept at 0.2 (internal phase) and 4 mL h^{-1} (outer phase). Then two internal streams were broken into a pair of drops that immediately incorporated into a larger biphasic one at the exit tips by the outer continuous phase. Ultimately, the hemisphere of CdS-loaded hybrid latex self-assembled into PC structure and was solidified after solvent evaporation. In contrast, the other hemisphere still existed in the liquid state. Therefore, solid−liquid Janus units were successfully achieved as the advanced building blocks, with the structural color confined in the solid hemisphere and superparamagnetic nanoparticles localized in the other liquid hemisphere.

Preparation of Molecular-Analogue Photonic Crystal Structures. Solid−liquid Janus building blocks could move directionally and generate coalescence of the liquid hemisphere upon collision under externally magnetic field, which thereby induced the formation of complex colloids with an adjustable number of solid protrusions. More interestingly, fluorescent PC clusters with hierarchical and anisotropic microarchitectures were further built via a surface-energy driven and photosensitive polymerized process.

Fabrication of PC Clusters via Magnetic Needle Arrays. To prepare PC clusters, hexagonal magnet arrays were fabricated by fixing 91 magnetic needles on a flat substrate with ethyl α-cyanoacrylate as instantaneous adhesive. After putting a polypropylene vessel containing Janus building blocks upon the magnet arrays, the liquid hemispheres of Janus building oriented toward the nearest magnet and moved to the corresponding magnet needle. When the Janus building blocks moved to the center of the magnetic field, the liquid hemispheres of these building blocks can collide and merge with each other into a larger hierarchical one. Subsequently, due to the minimization of surface energy, the solid compartments automatically formed a symmetrical structure on the liquid surface after removing the magnet arrays. The solid PC clusters with molecular-analogue structures can be obtained by the photopolymerization of liquid compartment under UV light (360 nm) for ∼10 s.

Preparation of Double-Display Patterns. A template of highly ordered circular hole arrays with uniform hole size of 250 μm and separation distance of 100 μm was fabricated through drilling an epoxy resin sheet (with thickness of 250 μm) with a numerical control machine tool. The magneto-controlled punctiform PC supraparticles with a diameter of 180 μm then were inserted into the holes covered by methylsilicone oil to form oil-filled cavities and sealed in the film with a thickness of 50 μm through pouring and curing of PDMS.

Characterizations. The optical images of the particles were taken using a SHUNYU SZM45 stereomicroscope with color CCD camera. Reflection spectra of Janus PC clusters were recorded using an optical microscope equipped with a fiber optic spectrometer (Ocean Optics,USB4000). Scanning electron microscopy (SEM) images were acquired on a QUANTA 200 (Philips-FEI, Holland) instrument at 20.0 kV. Fluorescent images were acquired with a Nikon inverted microscopy (ECLIPSE TE-2000U) equipped with a camera (Nikon, DS-U1). A 360 nm laser beam was chosen as the excited light source from an Xe-lamp with the tube voltage 550 V and the excitation and emission slits both 5 nm. Photoluminescence (PL) spectra were measured on a Varian Cary Eclipse spectrophotometer at room temperature. Transmission electron microscope (TEM) images were collected on a JEOL JEM-2100 transmission electron microscope. Fourier transform infrared (FT-IR) spectrum was recorded on a Nicolet 6700 FT-IR spectrometer and KBr crystal in the 400−4000 cm^{-1} region. Magnetization curves of homogeneous magnetic were performed on a Quantum DesignMPMS-XL7 SQUID magnetometer at 300 K.

RESULTS AND DISCUSSION

Figure 1 presents the entire preparative strategy for producing magnetic-fluorescent PC clusters. Well-defined poly(styrene-*co*-2-hydroxyethyl acrylate) (PS-*co*-PHEA) cores and poly(*N*-vinylimidazole-*co*-2-hydroxyethyl acrylate) (PVI-*co*-PHEA) shells were designed as microreactors for the fundamental carrier to fabricate CdS QDs-loaded hybrid latexes, enabling PC to have both photonic bandgap and fluorescent properties.[42] In the first step, we chose monodispersed PS-*co*-PHEA colloids as cores and poly(VI-*co*-HEA) hydrogels as shells to synthesize core−shell structural monodispersed colloids via seeded emulsion copolymerization (Figure S1). Taking advantage of the chelation of PVI within a shell to coordinate Cd^{2+},[43] CdS QDs with yellowish green fluorescence were in situ prepared within monodispersed microspheres after introducing a sulfur source (Na_2S) (Figure 1a and Figures S2, S3). Next, a triphase microfluidic device containing a parallel two-needle microchannel (providing channels for the discontinuous phases) and a tubular polydimethylsiloxane channel (providing channel for the continuous phase) was constructed, which allowed three liquid phases to flow simultaneously (Figure 1b). One of the discontinuous flowing phases was the as-prepared CdS-loaded hybrid latexes, and the other one was the photopolymerizable monomer EO_3-TMPTA containing 2 wt % superparamagnetic ferroferric oxide (Fe_3O_4) nanoparticles. The two discontinuous streams were broken into a pair of droplets, and then immediately incorporated into a larger single biphasic one at the exits of the parallel two-needle microchannel by an outer continuous phase of methylsilicone oil.

As advanced building blocks, a typical trait of Janus units is obvious double-faced geometry. Therefore, it is crucially important that the two immiscible phases in each droplet also show evident double-face structure in the creation of biphasic droplets. In this case, the shape of the biphasic droplets formed via the minimization of the interfacial free energy and the optimal surface tension of three phases. As shown in Figure S4, the geometry of a biphasic droplet depended on the balance of the triphase interfacial tensions, that is, the interfacial tension between methylsilicone oil and the solution of EO_3-TMPTA (γ_{ME}), the interfacial tension between methylsilicone oil and the aqueous solution of hybrid latexes (γ_{ML}), and the interfacial tension between the solution of hybrid latexes and EO_3-TMPTA (γ_{LE}). Herein, we modified the three-phase solution via surfactants to tune the values of interfacial tensions, where γ_{ME} = 6.1 mN m^{-1}, γ_{ML} = 8.8 mN m^{-1}, and γ_{LE} = 4.9 mN m^{-1}, and the geometry of biphasic droplets was thus designed to be obvious double-face structure. The straightforward investigation is displayed in Figure S5 and Movie S1. Ultimately, the hemisphere of hybrid latexes in the biphasic droplets self-assembled into PC structure with fluorescence and could be solidified after solvent evaporation. In contrast, the other magnetic hemisphere composed of EO_3-TMPTA and Fe_3O_4 nanoparticles still existed in the liquid state, retaining the mobility of the liquid. Consequently, solid−liquid Janus units were successfully achieved for the advanced building blocks, with the structural color and fluorescence confined in the solid hemisphere and superparamagnetic nanoparticles localize in the other liquid hemisphere.

The resulting Janus building block displayed restricted magnetic-responsive behavior under external magnetic field due to the presence of superparamagnetic Fe_3O_4 nanoparticles. As a small magnet was applied, the Janus building block moved

DOI: 10.1021/jacs.5b10039
J. Am. Chem. Soc. 2016, 138, 566−573

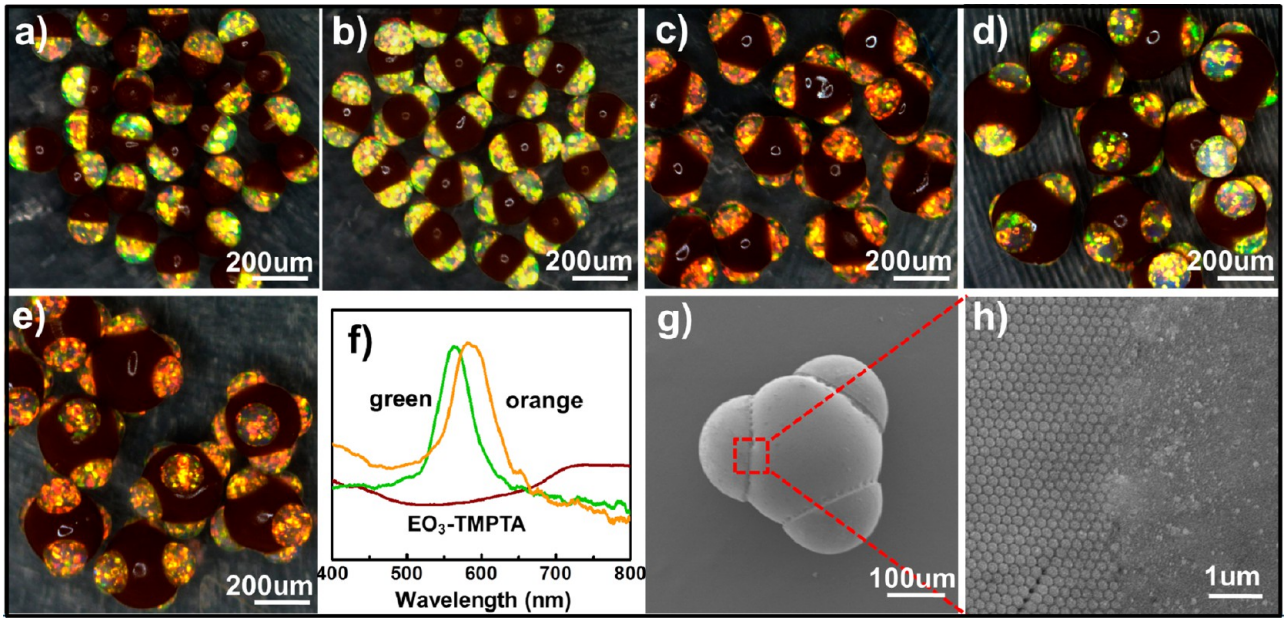

Figure 2. Optical and electron characterization of magnetic-fluorescent PC clusters. (a–e) Optical microscopy images of PC clusters, (a) AB_1, (b) AB_2, (c) AB_3, (d) AB_4, and (e) AB_5. (f) The reflection spectra of PC clusters: 562 nm for vertexal compartments s in AB_1, AB_2, and AB_4; 588 nm for vertexal compartments in AB_3 and AB_5; and no obvious peak for EO_3-TMPTA resins in all of the clusters. (g) SEM image of a typical triangular PC cluster. (h) High-resolution SEM image of the joint of the clusters.

to the external field and then rotated freely, facilitating the micromanipulation of liquid hemispheres direction and locomotion. Therefore, the liquid hemispheres of these Janus building blocks could collide and merge with each other into a larger hierarchical one with increased solid compartments via the pinpoint control of the center of the magnetic field (Figures 1c, S6). The simplified model can be expressed by eq 1:

$$A_1B_1 + A_1B_1 + \ldots\ldots + A_1B_1 = AB_n \quad (1)$$

where A is the liquid region, B is the solid compartment, and n is the number of Janus building block. The examples of diverse assembly pathways are presented in Figure 1c and Figure S7, within which a complex PC cluster could be derived from the original Janus unit or inferior PC clusters. During the combination process, the solid hemispheres retained their original fluorescence and photonic bandgap structure, while the liquid hemispheres converged into a bigger one. Thus, the final PC cluster was composed of a larger liquid part and multiple solid compartments, where the volume of the assembled liquid part was equal to n times the liquid part of single Janus building blocks. It should be noted that the solid PC compartments (part B) as individual vertexes were able to freely move on the surface of part A because of the liquid property of the A region. More importantly, due to the principle of lowest surface energy, the solid compartments (B) on the surface of the liquid (A) always formed the colloidal molecules with spherically symmetric distribution by magnetic-induced assembly. Also, the solid PC clusters with molecular-analogue structures can be shaped with a preliminarily expected configuration by exposing the colloidal molecules under UV light (360 nm) for about 10 s to polymerize liquid compartment. The SEM images and model structures of diverse molecular-analogue PC clusters are shown in Figure 1d and e, respectively. If the center of each PC compartment is regarded as a vertex of a polyhedron (Figure S8), the primer configurations can be denoted as AB_1 (dot, n = 1), AB_2 (line, n = 2), AB_3 (plane or triangle, n = 3), AB_4 (tetrahedron, n = 4), and AB_5 (triangular dipyramid, n = 5). Once $n \geq 4$, these configurations consisting of the vertices are deemed to be polyhedra or deltahedra, whose faces are equilateral triangles. These special structures appear in many common molecules, such as monatomic argon (Ar), diatomic hydrogen (H_2), boron trifluoride (BF_3), carbon tetrachloride (CCl_4), and phosphorus pentafluoride (PF_5). As illustrated in Figure 1e, the model morphologies quite match those obtained experimentally (Figure 1d), implying the final configuration of the complex PC clusters prepared from Janus building blocks via magnetic-directed assembly can be predicted and controlled. Notably, the route involved in this process is fairly simple to execute, facilitating its use in the preparation of complex particle materials with elaborate structures.

Figure 2 shows optical microscope and SEM images of anisotropic PC clusters with different frameworks. It is clearly seen that PC compartments displayed excellent uniformity at microscale with molecular-analogue microarchitectures, such as AB_1, AB_2, AB_3, AB_4, and AB_5 (Figure 2a–e). Also, it can be found that the PC clusters had regular and orderly structure with distinct structural color for PC multicompartments and reddish-brown for EO_3-TMPTA resin. This photonic bandgap structure is attributed to the periodic arrangement of monodispersed latexes, which would self-assemble into a close-packed PC structure after solvent evaporation. Figure S9 reveals the top- and cross-views of the PC compartments, clearly illustrating that the hybrid microspheres spontaneously organized into closely and regularly hexagon-packed structures in a long-range and maximal packing density. This ordered structure permeated the entire PC compartments from the surface to its center, indicating hexagonal close-packed lattice of latexes was still maintained after magnetic-directed assembly. Because the periodic arrangement of these monodispersed latexes will bring different reflection structural colors depending on the particle size of the latexes, the iridescent structural color of PC compartments can be facilely tuned via regulating the

DOI: 10.1021/jacs.5b10039
J. Am. Chem. Soc. 2016, 138, 566–573

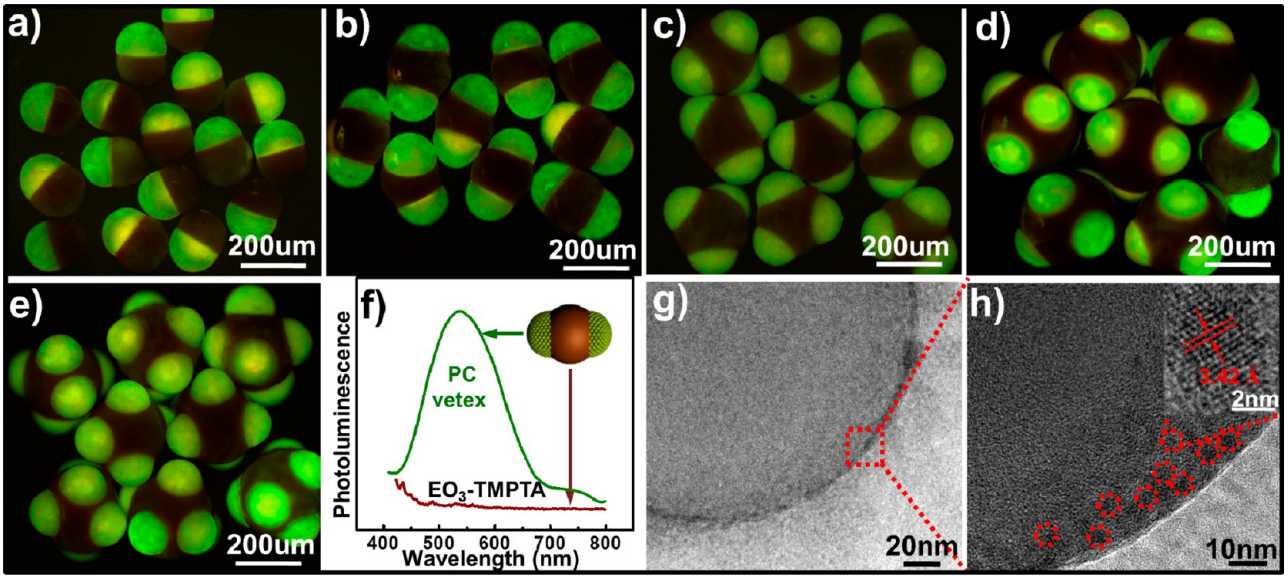

Figure 3. (a–e) Fluorescence microscopy images of PC clusters. (f) The corresponding PL spectra of vertexal compartments (λ_{em} = 540 nm) and EO_3-TMPTA resin (without fluorescence). (g,h) High-resolution transmission electron microscope (HRTEM) of a hydrogel microsphere loaded with CdS QDs (inset: a single CdS QDs with an excellent crystalline structure).

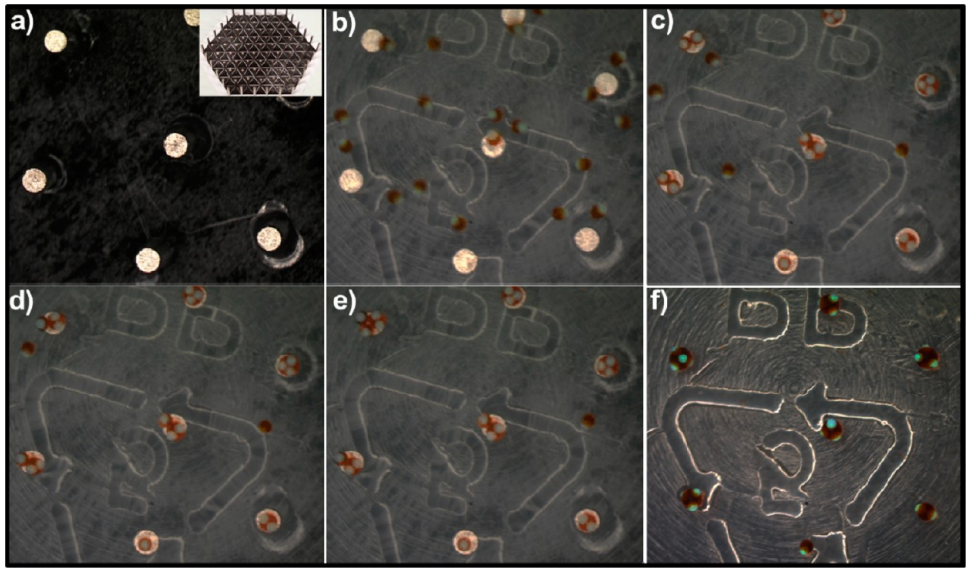

Figure 4. (a) Hexagonal arrays of magnetic needles adhered on a flat substrate. (b–e) The assembly process of solid–liquid Janus building blocks into PC clusters under magnet arrays. (f) Molecular-analogue PC clusters with spherically symmetric distribution after removing the magnet array (~30 s).

particle size of hybrid latexes. For instance, when the PC compartments were assembled from the hybrid latexes with the particle size at diameter of 226 nm, they showed yellow reflection color (Figure 2a, b, and d), but presented orange color with the latexes for the particle size at a diameter of 239 nm (Figure 2c and e). As shown in Figure 2f, the reflection peak with the wavelength of 563 nm corresponds to yellow color (PC compartments in AB_1, AB_2, and AB_4), while the wavelength of 588 nm represents orange color (PC compartments in AB_3 and AB_5). Unlike previously reported anisotropic particles, in which two component phases were diffused,[44] the as-prepared PC compartments were not only stably bonded to EO_3-TMPTA resins, but also presented a distinct boundary (Figure 2g). The high-magnification SEM image for the surface junction of PC clusters illuminates that the hybrid microspheres mainly form a hexagonal close-packed lattice and thus generate structural color in the PC compartment (Figure 2h).

The anisotropic characteristics also offer the possibility to produce PC clusters with multifunctional properties. Here, PVI-*co*-PHEA was used as a microreactor to in situ prepare CdS QDs in the hybrid latex (Figures 1a, S10, and S11). Figure 3a–e shows the fluorescent microscopy images of PC clusters encapsulated with CdS QDs. Bright yellowish green fluorescence emission was observed in the vertexes, but no fluorescence was found in EO_3-TMPTA resin, indicating successful preparation of CdS QDs in hybrid latexes. The corresponding photoluminescent (PL) spectra of vertexes and EO_3-TMPTA resin are presented in Figure 3f. In contrast to EO_3-TMPTA resin, an obvious broad peak centered at 540 nm indicated the recombination of surface electrons and holes of

DOI: 10.1021/jacs.5b10039
J. Am. Chem. Soc. 2016, 138, 566–573

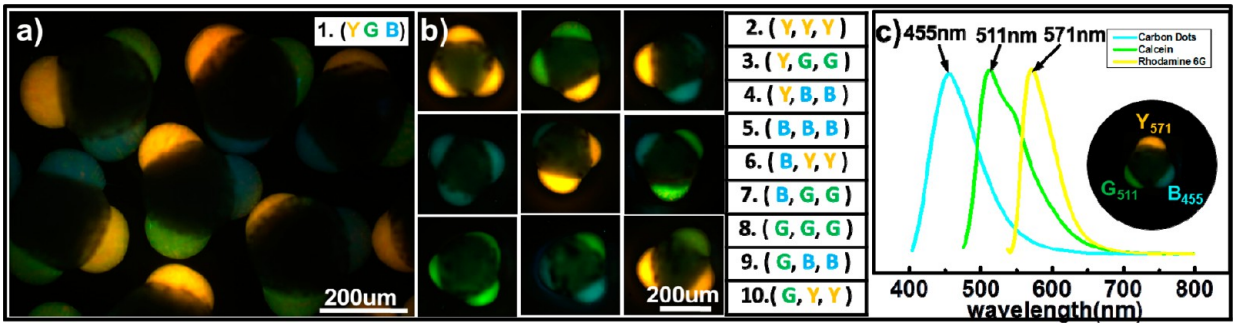

Figure 5. (a) Fluorescence microscopy images of triangular PC clusters assembled from Janus building blocks embedded with rhodamine 6G, calcein, and carbon dots, respectively. (b) Fluorescence microscopy images of nine types of PC clusters with different fluorescence color combinations. (c) PL spectra for the vertexes of triangular PC clusters assembled from Janus building blocks embedded with rhodamine 6G, calcein, and carbon dots, respectively. Inset: Fluorescence image of obtaining triangular PC clusters with bright yellow (Y571), green (G511), and blue (B455) fluorescence in vertexes.

CdS QDs in the PC compartment. Also, fluorescent properties of the QDs were well retained in the assembled clusters due to the excellent dispersion of CdS QDs. To further probe the dispersion of CdS QDs in the latex, a high-resolution transmission electron microscope (HRTEM) was employed. Figure 3g and h obviously shows a homogeneous distribution of CdS QDs without any aggregation in the shell of the hybrid microsphere. Moreover, well-resolved lattice fringes of CdS QDs (Figure 3h, inset) clearly show a perfect crystalline structure, which reveals the CdS QDs were well preserved in the hybrids. The interplanar spacing is 3.42 Å, which is corresponding to the (111) diffraction facet of CdS QDs.[45] These results confirm this procedure endows the PC compartments with fluorescence, opening an available way to realize the combination of electronic confinement originating from QDs and photonic bandgap of the PCs within a single structure.

To realize batch production of molecular-analogue photonic crystal structures, the magnet array was designed and applied for the organization of Janus building blocks. As described in Figure 4a and Figure S12, the magnetic needle array was immobilized on a flat substrate with the configuration of hexagonal modules. Because the Janus units can freely rotate under magnetic field, when the vessel containing solid–liquid Janus building blocks was placed on the magnet array (Figure 4b), the liquid hemispheres oriented toward the nearest magnet, driving the mobile of Janus units to the corresponding magnet needle. The Janus building blocks then met at the center of the magnetic field, and their liquid hemispheres collided and merged with each other into a larger hierarchical one (Figure 4c–e). The detail morphology of Janus building blocks before and after coalescence can be seen in Movie S2, in which the micromanipulation of liquid hemispheres direction and locomotion can be easily achieved under the external magnet array. After the magnet array was removed, the solid compartments on the surface of liquid always appeared as the colloidal molecules with spherically symmetric distribution (Figure 4f). This phenomenon can be attributed to the surface-energy-driven process, in which the colloidal clusters prepared by evaporating technology demonstrated a given number of spheres that followed the rule of the second moment of the mass distribution, $M_2 = \Sigma_{i=1}^{N} |\vec{r}_i - \vec{r}_0|^2$, where $\vec{r}_i$ is the center coordinate of the ith sphere and $\vec{r}_0$ is the center of mass of the cluster. In our colloidal system, interfacial tension forced the solid PC compartments to form clusters partially immersed in a liquid compartment, which is comparable to the late stage of droplet evaporation. Thus, a similar arrangement of PC compartments was found on the surface of the liquid as in Manoharan's work.[10] More importantly, through this principle and designed magnet array, the batch process of molecular-analogue photonic crystal clusters could be achieved (Figure S13). In addition, a computer numerical control (CNC) system could be promisingly designed in practice to fabricate PC clusters in an automated route (Figure S14). Details for the building of different kinds of PC clusters via CNC system have been provided in Figures S15–S18. Through these paradigmatic examples, it can be believed that diverse PC clusters could be systematically achieved in batch by facilely tuning the configuration of magnet array and the position of Janus building blocks.

Another advantage of triphase microfluidic technology is that it can fabricate particle materials with desired components and functions. To endow the PC clusters with additional performances, we achieved the generation of Janus building blocks with on-demand photonic bandgap and diverse fluorescent colors by encapsulating different chemical compositions into the expected solid hemisphere. In this process, three kinds of fluorescent substances, that is, rhodamine 6G, calcein, and carbon dots (CDs), were chosen to replace CdS QDs in polystyrene (PS) monodispersed latexes (238 nm), respectively, obtaining three types of Janus building blocks with bright yellow (Y), green (G), and blue (B) fluorescence. On the basis of these Janus building blocks, the triangular PC cluster can emit different fluorescence from three vertexes (Figure 5a). More interestingly, a serious combination model from these three Janus building blocks could be easily achieved in a pre-established manner. Taking the example of three vertexes (Figure 5a,b), 10 kinds of fluorescent emission from PC clusters, including (Y, G, B), (Y, Y, Y), (Y, G, G), (Y, B, B), (B, B, B), (B, Y, Y), (B, G, G), (G, G, G), (G, B, B), and (G, Y, Y) codes, can be accomplished. In addition, more combinations can be facilely gained by the introduction of more sorts of vertexes. The species of anisotropic PC clusters assembled from n Janus building blocks could be deduced by the following computational formula, eq 2:

$$N = C^1_n + C^2_n * C^1_{n-1} + C^3_n * C^1_{n-1} + \ldots\ldots + C^{n-1}_n * C^1_{n-1} + C^n_n \quad (2)$$

where N is the number of anisotropic PC clusters, and n is the number of PC vertexes within the PC cluster. Just as mentioned

DOI: 10.1021/jacs.5b10039
J. Am. Chem. Soc. 2016, 138, 566–573

above, triangular PC clusters have 10 kinds of hierarchical microarchitectures by altering the order of the three Janus building blocks with different fluorescent colors (Figure 5). Following this rule, tetrahedron PC clusters assembled from four different Janus building blocks will expand to 35 kinds of hierarchical microarchitectures, and triangular bipyramid PC clusters will reach a surprising 106 kinds of hierarchical microarchitectures. This encouraging encoding performance allows multiple fluorescence signals to be immediately and plentifully integrated into a single complex particle and to be easily decoded by the aid of fluorescence analysis equipment (Figure 5c), revealing the potential applications of PC clusters in biological coding and efficient information storage, as well as three-dimensional (3D) anticounterfeiting marks.

Interestingly, due to the small size and superparamagnetic nature (Figure S20), the PC clusters can be micromanipulated by a small magnet at various scales (Figure 6). As shown in

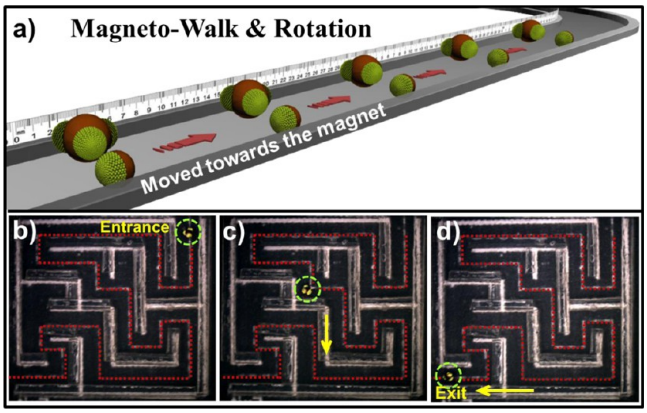

Figure 6. (a) Schematic representation showing a walking motion of magneto-controlled PC clusters. (b–d) Movement of triangular PC cluster for transmitting information under microscale labyrinth by magneto-controlled PC clusters. Details can be found in Figure S19 and Movie S3.

Figure 6a, a schematic representation indicates the as-prepared anisotropic PC clusters can directionally move along with external magnetic field. In a sense, the PC clusters can be regarded as a magneto-controlled robot, allowing them to be used for the information transmission. Herein, we took the triangular PC cluster as a typical robot, which can carry at least three kinds of fluorescent information to pass through intricate routes without direct touch.[46] The specific movement of the triangular robot carrier toward the direction of the magnetic field can be caught. As shown in Figure 6b–d and Movie S3, the anisotropic PC cluster walked smoothly through a microscopic labyrinth with a channel width of about 800 μm. Besides the motion, the orientation of the PC clusters can be also facilely controlled by applying an external magnetic field, resulting in a Janus PC particle or a triangular PC cluster with arbitrary rotation angles (Figure S21a, Movie S4, and Movie S5). Therefore, the PC clusters with well optical and magnetic responses could find wide applications in optical switches, bead display, and directed self-organized ordered colloidal lattice, etc. For example, a new kind of magneto-driven display panel with double-optical switch was achieved by imbedding the colorful Janus PC particles into highly ordered hole-arrays on a substrate, where the Janus PC particles could rotate freely through the acquirement of a dipole moment from external magnetic field. Importantly, each Janus particle can be regarded as an individual pixel, which was varied by alternating magnetic field, allowing the formation of a typical colorful fluorescent switch (Figure S21b). When the Fe_3O_4 nanoparticle compartments faced upward, the pixels showed a reddish-brown color under daylight and black color under UV light, respectively. Conversely, when the CdS-loaded PC hemispheres oriented upward, the pixels displayed vivid structural color under daylight and bright yellowish green fluorescence under UV light. More interestingly, on the basis of the feature of independent rotation, we could realize free-writing of these Janus particles on the panel using a magnetic needle. As indicated in Figures S21c,d, the letters of "C" and "N" were successfully displayed in the panel. Once a magnetic needle was actuated, the display panel easily made patterns, which can immediately return to the original state under reverse magnetic stimulation, showing rewritable use of the panel.

CONCLUSION

We have successfully established a robust strategy to fabricate a series of molecular-analogue photonic crystal structures with hierarchical microarchitectures based on solid–liquid Janus building blocks. The exceptional performance of these architectures presents a significant step toward construction of complex anisotropic particle materials with diverse geometries and versatile functions. The capability to precisely tune PC clusters into multiangular configurations (dot, line, triangle, and tetrahedron to triangular bipyramid) unlocks a vast potential for pipelined integration of photoelectricity material toward information communication. With this approach, we assert that various well-controlled molecular-analogue supraparticles can be designed and applied in anticounterfeiting, biolabeling, and information encoding.

ASSOCIATED CONTENT

Supporting Information

The Supporting Information is available free of charge on the ACS Publications website at DOI: 10.1021/jacs.5b10039.

Supplementary characterization details of Janus particles and clusters; detailed discussion on fluorescent characterization of the CdS-loaded hybrid latex, the balance of interfacial tensions between the three phases, real-time images of biphase droplets in triphase flow-focusing microfluidic device, mechanism of a magnetic-directed process for the fabrication of PC clusters, magnetic properties of PC clusters and computer numerical control (CNC), and magnet array used for fabricating PC clusters (PDF)

Movie S1, the fabrication of biphase droplets in a droplet-based triphase microfluidic device (ZIP)

Movie S2, the micromanipulation and coalescence of liquid hemispheres by magnet array (ZIP)

Movie S3, the magneto-walking of the PC clusters (ZIP)

Movie S4, the magneto-rotation of the typical Janus PC clusters (ZIP)

Movie S5, the magneto-rotation of the typical triangular PC clusters (ZIP)

AUTHOR INFORMATION

Corresponding Author

*chensu@njtech.edu.cn

Notes

The authors declare no competing financial interest.

DOI: 10.1021/jacs.5b10039
J. Am. Chem. Soc. 2016, 138, 566–573

■ ACKNOWLEDGMENTS

This work was supported by the Natural Science Foundation of China (21076103, 21176122, 21474052, and 21506095), the Natural Science Foundation of Jiangsu Province (BK20140934 and BK20150940), Priority Academic Program Development of Jiangsu Higher Education Institutions (PAPD), and the Qing Lan Project.

■ REFERENCES

(1) Pregibon, D. C.; Toner, M.; Doyle, P. S. *Science* **2007**, *315*, 1393−1396.
(2) Utada, A. S.; Lorenceau, E.; Link, D. R.; Kaplan, P. D.; Stone, H. A.; Weitz, D. A. *Science* **2005**, *308*, 537−541.
(3) Du, J.; O'Reilly, R. K. *Chem. Soc. Rev.* **2011**, *40*, 2402−2416.
(4) Hu, J.; Zhou, S.; Sun, Y.; Fang, X.; Wu, L. *Chem. Soc. Rev.* **2012**, *41*, 4356−4378.
(5) Kim, S. H.; Weitz, D. A. *Angew. Chem., Int. Ed.* **2011**, *50*, 8731−8734.
(6) Chu, L. Y.; Utada, A. S.; Shah, R. K.; Kim, J. W.; Weitz, D. A. *Angew. Chem., Int. Ed.* **2007**, *46*, 8970−8974.
(7) Tan, W. H.; Takeuchi, S. *Adv. Mater.* **2007**, *19*, 2696−2701.
(8) Maeda, K.; Onoe, H.; Takinoue, M.; Takeuchi, S. *Adv. Mater.* **2012**, *24*, 1340−1346.
(9) Glotzer, S. C.; Solomon, M. J. *Nat. Mater.* **2007**, *6*, 557−562.
(10) Manoharan, V. N.; Elsesser, M. T.; Pine, D. J. *Science* **2003**, *301*, 483−487.
(11) Damasceno, P. F.; Engel, M.; Glotzer, S. C. *Science* **2012**, *337*, 453−457.
(12) Whitesides, G. M.; Grzybowski, B. *Science* **2002**, *295*, 2418−2421.
(13) Rossi, L.; Sacanna, S.; Irvine, W. T. M.; Chaikin, P. M.; Pine, D. J.; Philipse, A. P. *Soft Matter* **2011**, *7*, 4139−4142.
(14) Henzie, J.; Grünwald, M.; Widmer-Cooper, A.; Geissler, P. L.; Yang, P. *Nat. Mater.* **2011**, *11*, 131−137.
(15) Li, F.; Josephson, D. P.; Stein, A. *Angew. Chem., Int. Ed.* **2011**, *50*, 360−388.
(16) Ejima, H.; Richardson, J. J.; Caruso, F. *Angew. Chem., Int. Ed.* **2013**, *52*, 3314−3316.
(17) Kraft, D. J.; Vlug, W. S.; van Kats, C. M.; van Blaaderen, A.; Imhof, A.; Kegel, W. K. *J. Am. Chem. Soc.* **2009**, *131*, 1182−1186.
(18) Chen, Q.; Bae, S. C.; Granick, S. *Nature* **2011**, *469*, 381−384.
(19) Yan, J.; Bloom, M.; Bae, S. C.; Luijten, E.; Granick, S. *Nature* **2012**, *491*, 578−581.
(20) Wang, T.; Zhuang, J.; Lynch, J.; Chen, O.; Wang, Z.; Wang, X.; LaMontagne, D.; Wu, H.; Wang, Z.; Cao, Y. C. *Science* **2012**, *338*, 358−363.
(21) Chen, Q.; Whitmer, J. K.; Jiang, S.; Bae, S. C.; Luijten, E.; Granick, S. *Science* **2011**, *331*, 199−202.
(22) Gao, W.; Pei, A.; Feng, X.; Hennessy, C.; Wang, J. *J. Am. Chem. Soc.* **2013**, *135*, 998−1001.
(23) Jones, M. R.; Mirkin, C. A. *Nature* **2012**, *491*, 42−43.
(24) Wang, Y.; Wang, Y.; Breed, D. R.; Manoharan, V. N.; Feng, L.; Hollingsworth, A. D.; Weck, M.; Pine, D. J. *Nature* **2012**, *491*, 51−55.
(25) Wang, Y.; Hollingsworth, A. D.; Yang, S. K.; Patel, S.; Pine, D. J.; Weck, M. *J. Am. Chem. Soc.* **2013**, *135*, 14064−14067.
(26) Maye, M. M.; Nykypanchuk, D.; Cuisinier, M.; van der Lelie, D.; Gang, O. *Nat. Mater.* **2009**, *8*, 388−391.
(27) Zhang, G.; Wang, D.; Möhwald, H. *Angew. Chem., Int. Ed.* **2005**, *44*, 7767−7770.
(28) Gröschel, A. H.; Schacher, F. H.; Schmalz, H.; Borisov, O. V.; Zhulina, E. B.; Walther, A.; Müller, A. H. E. *Nat. Commun.* **2012**, *3*, 710.
(29) Gröschel, A. H.; Walther, A.; Löbling, T. I.; Schmelz, J.; Hanisch, A.; Schmalz, H.; Müller, A. H. E. *J. Am. Chem. Soc.* **2012**, *134*, 13850−13860.
(30) Gröschel, A. H.; Walther, A.; Löbling, T. I.; Schacher, F. H.; Schmalz, H.; Müller, A. H. E. *Nature* **2013**, *503*, 247−251.
(31) Tang, C.; Zhang, C.; Sun, Y.; Liang, F.; Wang, Q.; Li, J.; Qu, X.; Yang, Z. *Macromolecules* **2013**, *46*, 188−193.
(32) McConnell, M. D.; Kraeutler, M. J.; Yang, S.; Composto, R. J. *Nano Lett.* **2010**, *10*, 603−609.
(33) Kim, S. H.; Jeon, S. J.; Yi, G. R.; Heo, C. J.; Choi, J. H.; Yang, S. M. *Adv. Mater.* **2008**, *20*, 1649−1655.
(34) Kim, S. H.; Jeon, S. J.; Jeong, W. C.; Park, H. S.; Yang, S. M. *Adv. Mater.* **2008**, *20*, 4129−4134.
(35) Kim, S. H.; Park, J. G.; Choi, T. M.; Manoharan, V. N.; Weitz, D. A. *Nat. Commun.* **2014**, *5*, 3068.
(36) Zhao, Y.; Gu, H.; Xie, Z.; Shum, H. C.; Wang, B.; Gu, Z. *J. Am. Chem. Soc.* **2013**, *135*, 54−57.
(37) Velev, O. D.; Lenhoff, A. M.; Kaler, E. W. *Science* **2000**, *287*, 2240−2243.
(38) Ye, B.; Ding, H.; Cheng, Y.; Gu, H.; Zhao, Y.; Xie, Z.; Gu, Z. *Adv. Mater.* **2014**, *26*, 3270−3274.
(39) Yin, S. N.; Wang, C. F.; Liu, S. S.; Chen, S. *J. Mater. Chem. C* **2013**, *1*, 4685−4690.
(40) Xie, Z.; Cao, K.; Zhao, Y.; Bai, L.; Gu, H.; Xu, H.; Gu, Z. Z. *Adv. Mater.* **2014**, *26*, 2413−2418.
(41) Liu, S. S.; Wang, C. F.; Wang, X. Q.; Zhang, J.; Tian, Y.; Yin, S. N.; Chen, S. *J. Mater. Chem. C* **2014**, *2*, 9431−9438.
(42) Zhang, J.; Ling, L.; Wang, C. F.; Chen, S.; Chen, L.; Son, D. Y. *J. Mater. Chem. C* **2014**, *2*, 3610−3616.
(43) Tu, J.; Zhou, J.; Wang, C. F.; Zhang, Q.; Chen, S. *J. Polym. Sci., Part A: Polym. Chem.* **2010**, *48*, 4005−4012.
(44) Yin, S. N.; Wang, C. F.; Yu, Z. Y.; Wang, J.; Liu, S. S.; Chen, S. *Adv. Mater.* **2011**, *23*, 2915−2919.
(45) Yang, S. Y.; Li, Q.; Chen, L.; Chen, S. *J. Mater. Chem.* **2008**, *18*, 5599−5603.
(46) Morin, S. A.; Shepherd, R. F.; Kwok, S. W.; Stokes, A.; Nemiroski, A.; Whitesides, G. M. *Science* **2012**, *337*, 828−832.

DOI: 10.1021/jacs.5b10039
J. Am. Chem. Soc. 2016, 138, 566−573